analytical chemistry

ARTICLE

pubs.acs.org/ac

Method for Determination of Peak Areas in Nonequilibrium Capillary Electrophoresis of Equilibrium Mixtures

Leonid T. Cherney, Mirzo Kanoatov, and Sergey N. Krylov*

Department of Chemistry and Centre for Research on Biomolecular Interactions, York University, Toronto, Ontario M3J 1P3, Canada

Supporting Information

ABSTRACT: Nonequilibrium capillary electrophoresis of equilibrium mixtures (NECEEM) facilitates determination of both the kinetic constants (k_{off}) and the equilibrium constants (K_d) of complex dissociation from a single experiment. A typical NECEEM electropherogram consists of two peaks and an "exponential bridge" between them, smoothly merging into the peaks. The values of k_{off} and K_d are usually calculated with simple algebraic formulas, by utilizing the areas of the peaks and the bridge. Accurate determination of the two constants requires accurate positioning of the two boundaries separating the bridge from the peaks. Here, we propose a more systematic method for the determination of boundaries between the peaks and the bridge. The method involves a simple geometrical analysis of a NECEEM electropherogram based on an assumption of symmetry in ordinary electrophoretic peaks. To test the method, we (i) constructed a series of computer-simulated NECEEM electropherograms, (ii) determined the two boundaries with our method, and (iii) calculated the values of k_{off} and K_d. We found that the deviation of the calculated values from those used to simulate the electropherograms did not exceed 15% for k_{off} and 25% for K_d, as long as the peaks and the bridge were visually identifiable. We finally applied the method to the determination of K_d and k_{off} values for the interaction between AlkB protein and its DNA aptamer. The developed method for rational boundary determination in NECEEM will facilitate accurate data analysis in a simple and efficient manner.

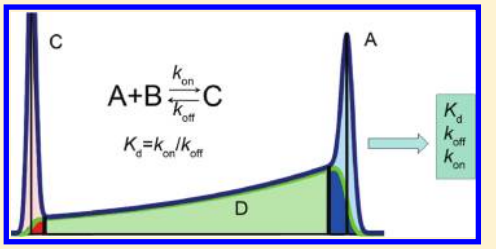

Many biological macromolecules assemble into noncovalent complexes for their proper function. Such complexes play an important role in key cellular processes including DNA replication, gene expression, signal transduction, transport across membranes, cell movement, enzyme maturation, etc.[1] Uncontrolled aggregation of misfolded proteins is known to result in pathological conditions (for example, in prion and amyloid diseases).[2] The kinetic and equilibrium stability of noncovalent complexes is characterized by the rate constant (k_{off}) and the equilibrium constant (K_d) of complex dissociation. Knowledge of both parameters is important for understanding the dynamics of the interaction and the role of noncovalent macromolecular complexes in cellular processes.

Several approaches have been developed to measure the rate constants of complex formation and dissociation.[3−10] Some of them, such as fluorescence correlation spectroscopy and nanopore amperometry, are microscopic in their nature and require observation of a statistically insignificant number of molecules.[4] Others, such as surface-immobilized binding sensors[5] and kinetic capillary electrophoresis (KCE) methods,[6−10] are macroscopic in their nature and require the measurement of changes in concentrations. Each of these approaches has different advantages, limitations, and major applications. KCE methods are particularly attractive when one of the reactants can be fluorescently labeled for detection without affecting the interaction. KCE methods can be used to measure a wide range of rate and equilibrium constants with only minute consumption of materials.

Nonequilibrium capillary electrophoresis of equilibrium mixtures (NECEEM) is one of the KCE methods. It is used more often than others, because of the simplicity of both the experiment and the data processing.[6−8] Other KCE methods (such as SweepCE, plug−plug KCE, short SweepCEEM, and continuous NECEEM) require implementation of more-complex initial conditions or larger amounts of reactants than NECEEM does.[9,10] NECEEM was successfully applied to kinetic studies of protein−DNA,[11] protein−peptide,[12] and other macromolecular complexes.[13] It was also used for calibration-free quantitative analysis of proteins, using aptamers as affinity probes.[14−16] In addition, NECEEM has been proven to serve as a highly efficient partitioning approach in the selection of DNA aptamers.[14,16,17] Conceptually, NECEEM starts with mixing and equilibration of reactants A and B to allow the formation of their noncovalent complex, C:

$$A + B \underset{k_{off}}{\overset{k_{on}}{\rightleftharpoons}} C \qquad K_d = \frac{k_{off}}{k_{on}} = \frac{A_0 B_0}{C_0} \tag{1}$$

where A_0, B_0, and C_0 represent the equilibrium concentrations of A, B, and C, respectively. A short plug of the equilibrium mixture is then injected into a capillary and an electric field is applied to separate the three components via capillary electrophoresis. It is assumed that electrophoretic zones of A and B are separated fast so that the forward process in eq 1 is negligible, with respect to the reverse one. As a result, A and/or B are separated from C under nonequilibrium conditions and C continuously dissociates

Received: August 6, 2011
Accepted: October 13, 2011

dx.doi.org/10.1021/ac2027113 | *Anal. Chem.* XXXX, XXX, 000–000

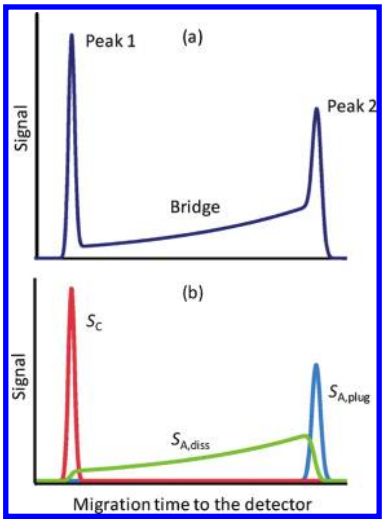

Figure 1. Graphical analysis of NECEEM data: (a) signal in a typical NECEEM electropherogram, and (b) signal deconvolution into its three components.

into A and B during the course of electrophoresis. Detection is typically arranged so that only one reactant (for example, A) and the complex C (C = AB) are visible (e.g., by fluorescently labeling A). In this case, a NECEEM electropherogram, which is, per se, signal versus migration time to a detector, contains three characteristic features: two peaks and a bridge between them that smoothly merges into the peaks (see Figure 1a). This cumulative signal (S) is a sum of three component signals: (i) signal generated by A that was unbound in the injected plug ($S_{A,plug}$), (ii) signal generated by A which was dissociated from C during electrophoresis ($S_{A,diss}$), and (iii) signal generated by C that reached the detector intact (S_C) (see Figure 1b).[8] $S_{A,plug}$ and S_C are major contributors to the two peaks, while $S_{A,diss}$ is the major contributor to the bridge in the electropherogram. Importantly, $S_{A,diss}$ overlaps at its flanks with $S_{A,plug}$ and S_C and thus merges the bridge flanks into the peaks. This overlap can create a challenge for accurately finding k_{off} and K_d from a NECEEM electropherogram and, therefore, is a reason for this study and its major subject.

The overlap does not impose a problem if a pattern-based approach is used to find k_{off} and K_d. In this approach, the constants are determined by fitting computer-simulated electropherograms into experimental ones.[8] While, arguably, being very accurate, the pattern-based approach is complicated and, thus, has not been utilized by practical users of NECEEM. Indeed, curve fitting is not a computatively transparent procedure that, generally speaking, depends on the initial curve used in fitting and may require significant computing time.[8]

In contrast, the overlap does create a challenge when a parameter-based approach is used to calculate k_{off} and K_d from a NECEEM electropherogram. The parameter-based approach utilizes the distinct features in a NECEEM electropherogram: areas under $S_{A,diss}$, $S_{A,plug}$, and S_C and the time position of maximum of S_C.[7,8] The areas and time should be determined from a NECEEM electropherogram, as shown in Figure 1a. Since the area under $S_{A,diss}$ partially overlaps with the areas under $S_{A,plug}$ and S_C (Figure 1b), determination of these three areas is not trivial. Generally, it requires deconvolution of the cumulative signal $S(t)$ into three components. Inaccurate deconvolution can result in inaccurate determination of k_{off} and K_d in the parameter-based approach. So far, the overlap of the areas in NECEEM electropherograms has been neglected, and the determination of the three areas has been done by visually placing vertical boundaries between the bridge and the peaks.[7] Subjective boundary positioning is influenced by individual judgment and experience of the analyst and leads to uncertainties in the determined k_{off} and K_d values. To exclude these uncertainties, a method is needed for rational and accurate determination of the overlapping areas. There are many studies on peak deconvolution in chromatography and electrophoresis.[18,19] Peak deconvolution has certain limitations and requires some preliminary knowledge about the individual peak shapes that are yet to be determined. For example, the application of integral transformations can be useful in peak deconvolution if individual signals are not considerably different in shape and are relatively narrower than the cumulative signal.[18] Evidently, this is not true for NECEEM signals (Figure 1). Deconvolution by curve fitting is based on known or hypothetical forms of the individual peaks.[19] In fact, the incorporation of such technique in NECEEM amounts to the use of the pattern-based approach. Indeed, the latter itself is based on fitting of the sum of three analytical solutions of the mass-transfer equations (see expressions (S5)−(S7) in the Supporting Information) into the cumulative signal. Therefore, a simpler and more straightforward method for the analysis of overlapping zones is needed for the parameter-based approach.

Here, we propose a systematic method for the determination of the areas under $S_{A,plug}$, $S_{A,diss}$, and S_C through the rational positioning of boundaries to account for the overlap of $S_{A,diss}$ with $S_{A,plug}$ and S_C. This analysis uses a general assumption of axial symmetry of $S_{A,plug}$ and S_C. Such an assumption is typically valid if neither A nor C adsorbs to inner capillary walls, and if the sample and run buffers are identical. To determine the accuracy of our method, we constructed a series of over 30 computer-simulated NECEEM electropherograms with a wide range of k_{off} and K_d values, determined the boundary positions with our method, and calculated K_d and k_{off} using the algebraic formulas previously derived. We found that the constants determined in this way deviated from those used in construction of the simulated electropherograms by no more than 15% for k_{off} and 25% for K_d for 90% of the electropherograms. We expect that the proposed method will be very useful in fast data analysis of NECEEM experiments.

RESULTS AND DISCUSSION

Basic Equations for Parameter-Based Approach to k_{off} and K_d Determination in NECEEM. Since the injected plug contains the equilibrium mixture of A, B, and C, the following relations occur in the injected plug before separation begins:

$$a_0 b_0 = V K_d c_0, \quad a_0 + c_0 = a_{tot}, \quad b_0 + c_0 = b_{tot} \qquad (2)$$

Here, a_0, b_0, and c_0 are total equilibrium amounts of A, B, and C, respectively, in the plug; V is the plug volume; and a_{tot} and b_{tot} are total amounts of A and B used to prepare the plug (without adding any amount of C). The first relation in Expression 2 represents the law of mass action. The other two relations in Expression 2 express the mass balance between A, B, and C in reaction 1. The total amount $c(t)$ of complex C decreases with time, according to the following law:[8]

$$c(t) = c_0 \exp(-k_{off} t) \qquad (3)$$

dx.doi.org/10.1021/ac2027113 |Anal. Chem. XXXX, XXX, 000–000

Equation 3 results from general equations of mass transfer in the NECEEM approximation of negligible forward process (see the Supporting Information). Expressions 2 and 3 allow us to express K_d and k_{off} and in terms of quantities that either are known or can be easily measured:[8]

$$K_d = \frac{(b_{tot}/V)[1 + (a_0/c_0)] - (a_{tot}/V)}{1 + (c_0/a_0)}, \quad k_{off} = \left(\frac{1}{t_C}\right) \ln\left(\frac{c_0}{c(t_C)}\right) \tag{4}$$

where t_C is the migration time of the maximum concentration of intact C to the detector. Ratios a_{tot}/V and b_{tot}/V are usually known, since they are the initial concentrations of A and B immediately after mixing A and B and before the appreciable formation of C. These nonequilibrium concentrations should not be confused with the equilibrium ones (A_0 and B_0) that are unknown in the NECEEM setup. Expressions 4 allows one to find K_d and k_{off}, since the value of a_0/c_0, $c_0/c(t_C)$, and t_C can be determined using a NECEEM electropherogram. Provided that values of K_d and k_{off} are found, the rate constant k_{on} can be calculated directly, using the second relation in eq 1.

Expressions 4 contains total amounts (a_0, c_0, and $c(t_C)$) of components A and C, whereas the experimental data, such as electropherograms, operate with signals (optical, electrochemical, etc.). To express a_0, c_0, and $c(t_C)$ in terms of measurable areas of characteristic regions of the electropherograms, we assume that signals of visible components are proportional to their concentrations:

$$S_A = g_A A, \quad S_C = g_C C \left(\text{where } g_A = \frac{Q_A}{\chi_A}, g_C = \frac{Q_C}{\chi_C}\right) \tag{5}$$

In relations 5, S_A and S_C are the signals generated by A and C, respectively; A and C represent the local concentrations of A and C (defined as their amounts per unit length of the capillary), respectively. In the case of fluorescence detection, the coefficients g_A and g_C are given by the expressions in the brackets in relations 5, where Q_A and Q_C are the absolute quantum yields of A and C, and χ_A and χ_C are proportionality coefficients.[20,21] As previously noted, the cumulative signal S in a NECEEM electropherogram (see Figure 1a) can be presented as a sum of the three component signals (see Figure 1b):

$$S = S_{A,plug} + S_{A,diss} + S_C \tag{6}$$

Relations 5 and 6 allow the ratios a_0/c_0 and $c_0/(c(t_C))$ to be expressed in terms of measurable characteristic features of the cumulative signal S (see the Supporting Information):

$$\frac{a_0}{c_0} = \frac{\Omega(A) - \Omega(A^*)}{G(\Omega(C) - \Omega(C^*)) + \Omega(D) + \Omega(A^*) + \Omega(C^*)} \tag{7}$$

$$\frac{c_0}{c(t_C)} = 1 + \frac{\Omega(D) + \Omega(A^*) + \Omega(C^*)}{G(\Omega(C) - \Omega(C^*))} \tag{8}$$

Here, $\Omega(A)$ is the area of the A peak, and $\Omega(A^*)$ is the area of the overlapping zone A* between the A peak and the zone under $S_{A,diss}$ (see Figures 2a and 2b). Similarly, $\Omega(C)$ is the area of the C peak, and $\Omega(C^*)$ is the area of the overlapping zone C* between the C peak and the zone under $S_{A,diss}$. Finally, $\Omega(D)$ is the area of zone D under $S_{A,diss}$ without the overlapping zones (see Figures 2a and 2b). The A peak and zone A* start at the beginning of signal $S_{A,plug}$, whereas the C peak and zone C* end at the end of signal S_C.

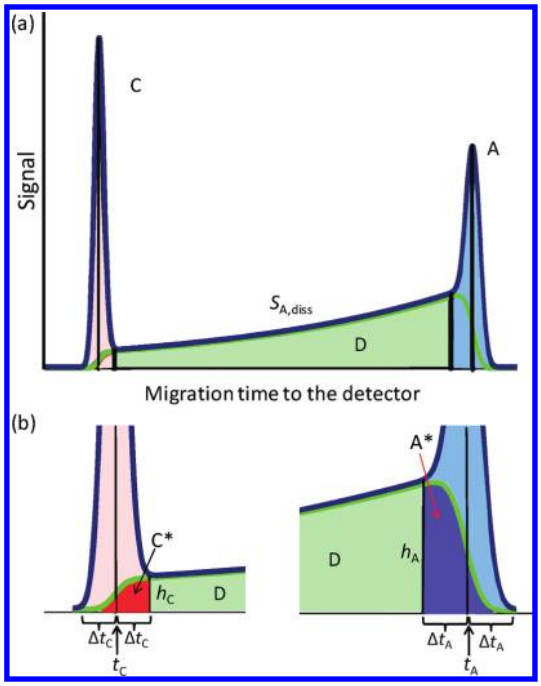

Figure 2. Identification of areas used for calculation of K_d and k_{off}: (a) typical NECEEM electropherogram from Figure 1a with areas $\Omega(A)$, $\Omega(C)$, and $\Omega(D)$ shown in blue, pink, and green colors, respectively (upper boundaries of the overlapping zones A* and C* are shown by the green color); and (b) details of the overlapping zones. Areas $\Omega(A^*)$ and $\Omega(C^*)$ are shown by dark blue and dark red colors, respectively. The time interval from the beginning of the C peak to its maximum (t_C) is denoted by Δt_C. Similarly, Δt_A is the time interval from the maximum of the A peak (t_A) to the its end. The bases of the overlapping zones C* and A* are equal to $2\Delta t_C$ and $2\Delta t_A$, respectively. The heights of the overlapping zones are denoted by h_C and h_A. They coincide with boundaries between zone D and the C and A peaks, respectively.

In eqs 7 and 8, parameter G is determined by the following relation (also see the Supporting Information):

$$G = \frac{g_A \nu_C}{g_C \nu_A} = \frac{\chi_C Q_A t_A}{\chi_A Q_C t_C} \tag{9}$$

where the migration times of the A and C peaks (t_A and t_C, respectively) can be readily determined from their positions in NECEEM electropherograms (see the Supporting Information).

Now we need to determine the boundaries of the A and C peaks and $\Omega(A^*)$ and $\Omega(C^*)$. To do this, we assume that peaks $S_{A,plug}$ and S_C are symmetrical (see Figure 1b) and that the time positions of their maxima approximately coincide with those of the maxima of the A and C peaks. In this case, the bases of the A peak and overlapping zone A* are equal to $2\Delta t_A$ (see Figure 2b). Here, Δt_A is a time interval between the end of the A peak and the time t_A of the maximum of A. Similarly, the bases of the C peak and overlapping zone C* are equal to $2\Delta t_C$ (see Figure 2b). Here, Δt_C is the time interval between the time t_C of the maximum of the C peak and its beginning. Obviously, the upper boundaries of the overlapping zones A* and C* coincide with the parts of the signal $S_{A,diss}$ located inside the A and C peaks, respectively (see Figure 2a). Polynomial approximation of these boundaries gives

dx.doi.org/10.1021/ac2027113 |Anal. Chem. XXXX, XXX, 000–000

the following expressions (see the Supporting Information):

$$\Omega(A^*) = \left(\frac{2}{3}\right) h_A \Delta t_A, \quad \Omega(C^*) = \left(\frac{2}{3}\right) h_C \Delta t_C \tag{10}$$

where h_A and h_C are the heights of zones A* and C*, respectively.

In these calculations, we define time positions of the end of the A peak ($t_{A,end}$) and the start of the C peak ($t_{C,start}$) using the following conditions:

$$S - S_0 = 10^{-2} \max_A (S - S_0) \quad \text{at } t = t_{A,\,end}$$
$$= t_A + \Delta t_A \tag{11}$$

$$S - S_0 = 10^{-2} \max_C (S - S_0) \quad \text{at } t = t_{C,\,start}$$
$$= t_C - \Delta t_C \tag{12}$$

where S_0 is the level of the background in a NECEEM electropherogram for S. The determination of Δt_A, Δt_C, h_A, and h_C can be performed manually by measuring these values from graphically recorded (printed) NECEEM electropherograms. However, this determination can be made much more precisely using Microsoft Excel software to process the digitally recorded data (i.e., to find maxima of peaks, their starts and ends, etc.), as was done for all examples in this paper. Finally, $\Omega(A)$, $\Omega(C)$, and $\Omega(D)$ can be easily found from the total signal, since the boundaries between the A and C peaks and the zone D are determined by vertical lines (see Figure 2a). As long as all of the necessary areas can be found, relations 4 and eqs 7−9 allow one to determine K_d and k_{off} easily. A tutorial example of such calculations for a real experimental electropherogram of the AlkB-DNA complex is given in the Supporting Information.

Accuracy of the New Systematic Method for Boundary Positioning. It is instructive to estimate the accuracy of the developed systematic method for boundary positioning. The most effective way for this is to study relative errors in the calculations of a_0, c_0, and $c(t_C)$. Indeed, these component amounts are directly expressed through the characteristic areas (in signals) defined by boundary positioning, whereas values of K_d and k_{off} themselves are determined by a_0, c_0, and $c(t_C)$. To carry out such accuracy analysis, we must analyze NECEEM electropherograms for reaction 1 at various *known* values of K_d, k_{off}, a_0, and c_0. The best way to produce such electropherograms is to simulate them using the exact NECEEM solution for equations of mass transfer (see the Supporting Information).[8,9] This solution holds true as long as the forward reaction is negligible, with respect to the reverse reaction in eq 1. A computer program, utilizing the exact analytical NECEEM solution, allows one to calculate $S_{A,plug}$, $S_{A,diss}$, and S_C, as well as their sum S for varying K_d, k_{off}, a_0, and c_0.[8] Then, the simulated electropherogram (S versus time) can be used to back-calculate a_0, c_0, and also $c(t_C)$, using expressions (S9)−(S12) in the Supporting Information. Since the true values of a_0, c_0, and $c(t_C)$ (where $c(t_C) = \int C(t_C)\,dx$) are known in this case, the corresponding relative errors (an absolute value of the ratio between the deviation from the true value and the true value) are easily determined. After that, relative errors for K_d and k_{off} can be calculated, as shown in the Supporting Information. Alternatively, we can determine values of a_0, c_0, $c(t_C)$, K_d, and k_{off} and the corresponding relative errors, if the visual method for boundary positioning is employed. In this method, overlapping zones are neglected and the boundaries are assumed to be vertical lines positioned visually.

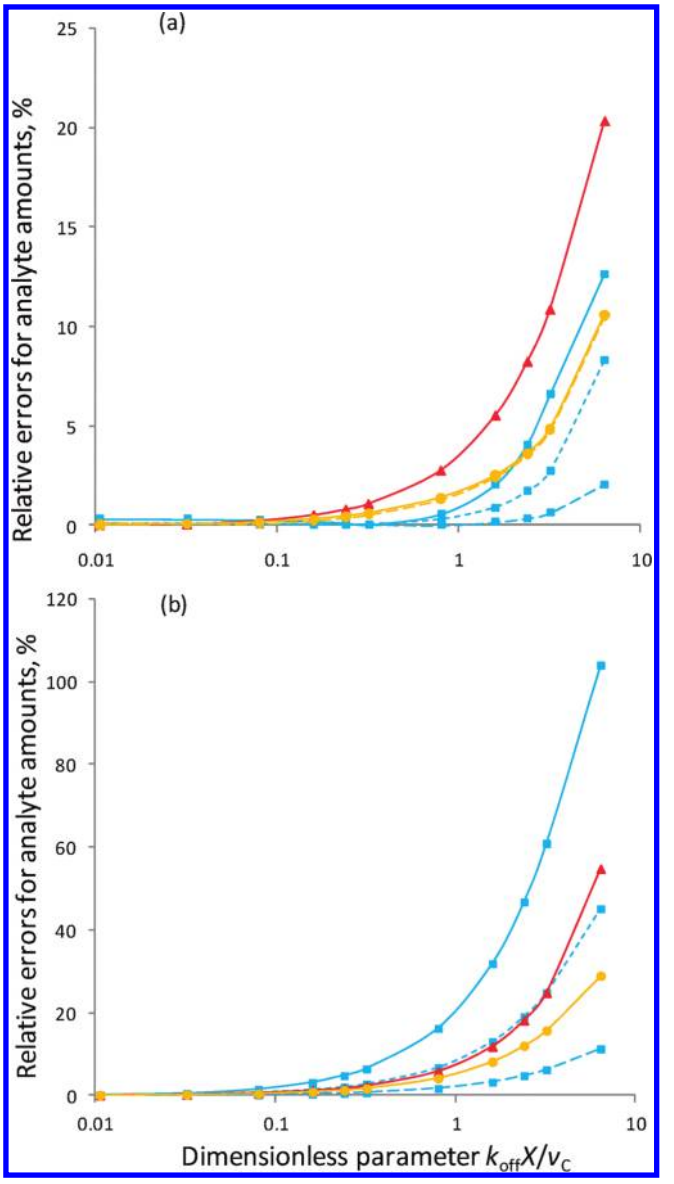

Figure 3. Relative errors in the determination of a_0, c_0, and $c(t_C)$ versus dimensionless parameter $k_{off}X/v_C$ for the (a) systematic and (b) visual methods of boundary positioning. Dependencies for a_0, c_0, and $c(t_C)$ are depicted by blue, orange, and red colors, respectively. Solid lines show errors for ratio $K_d/B_0 = 0.2$. Short and long dashed lines correspond to values $K_d/B_0 = 0.5$ and $K_d/B_0 = 2.0$, respectively. Dashed lines for c_0 and $c(t_C)$ are almost indistinguishable from the corresponding solid lines.

We simulated a total of 33 NECEEM electropherograms mimicking experimental ones. They corresponded to various values of K_d, k_{off}, a_0, and c_0. The values of the velocities, the initial plug width W, and the detector position X were given as

$$v_C = 0.12\text{cm/s}$$

$$v_A = 0.08\text{cm/s}$$

$$W = 0.36\text{cm}$$

$$X = 40\text{cm}$$

dx.doi.org/10.1021/ac2027113 |*Anal. Chem.* XXXX, XXX, 000–000

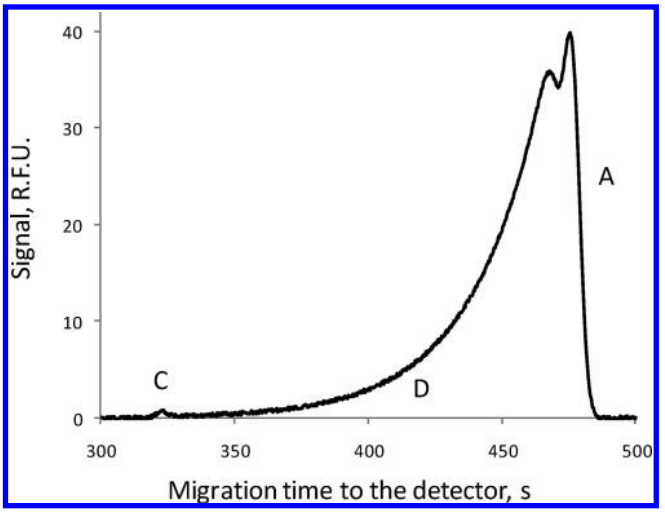

Figure 4. Signal simulated with the exact NECEEM solution at $k_{off}X/v_C$ = 5.75 and K_d/B_0 = 0.2.

which are typical for NECEEM experiments. For simplicity, we assumed that the coefficients in signal−concentration relations are the same: $g_A/g_C = 1$. Some representative simulated electropherograms are shown in the Supporting Information.

Figure 3a shows relative errors in determination of the equilibrium amounts a_0 and c_0 of components A and C in the initial plug if the systematic method for boundary positioning is applied (overlapping zones are taken into account). This figure also demonstrates the relative errors in the determination of the amount $c(t_C)$ of complex C that reaches the detector. The accuracy of k_{off} determination is better than 4% in 32 simulations, and it reaches 14% in only one simulation (see Figure S5 in the Supporting Information). The accuracy of K_d determination is better than 15% in 29 simulations, and it lies in the range of 25%−50% only in four simulations (see Figure S5 in the Supporting Information). In contrast, Figure 3b shows relative errors in the determination of a_0, c_0, and $c(t_C)$ if the visual method for boundary positioning is used (overlapping zones are neglected). In this case, the corresponding values of k_{off} and K_d are found with significantly higher errors that can reach 500% for K_d (see Figure S5 in the Supporting Information). Figure 3 and Figure S5 in the Supporting Information clearly demonstrate the superiority of the developed systematic method to the visual one. At small and moderate values of $k_{off}X/v_C$, the former leads to errors that are several times smaller than those produced by the latter. At higher values of $k_{off}X/v_C$, the systematic method can give up to 10-fold reduction in errors for K_d: from 100%−500% to 25%−50% (Figure S5 in the Supporting Information). Furthermore, the systematic method is not dependent on a visual estimation of boundary position and, therefore, is less prone to user bias.

Note that the appearance of the exponential-like increase in errors in Figure 3 is caused by the logarithmic scale used for the horizontal axes. The actual dependences of the relative errors shown in this figure on $k_{off}X/v_C$ are practically linear. The higher end of the range of $k_{off}X/v_C$ in Figure 3 corresponds to the case of almost complete dissociation of the complex before it reaches the detector. Indeed, eq 3 yields a value of $c(t_C)/c_0 \approx 10^{-4}$ at $k_{off}X/v_C \approx 10$. As a result, the C peak in the simulated signal becomes many times smaller than the A peak that, in turn, acquires the second maximum (see Figure 4). Any further significant increase in $k_{off}X/v_C$ leads to the merger of the maxima of the A peak and to a fast decrease in the height of zone D at almost all distances from the A peak. As a result, the A peak tends to become almost symmetrical. Such behavior of the electropherogram leads to an increase in relative error in the determination of a_0, c_0, and $c(t_C)$ at the upper limit of the $k_{off}X/v_C$ range (recall Figure 3). In general, errors can result from (i) the approximate nature of modeling of the overlapping zone boundaries by the quadratic functions, (ii) the uncertainty in positioning the start and the end of the C and A peaks, respectively, and (iii) errors in the determination of peak maxima based on a single cumulative-signal electropherogram.

CONCLUDING REMARKS

In this work, we introduced a systematic method for finding boundary positions between three characteristic parts of nonequilibrium capillary electrophoresis of equilibrium mixture (NECEEM) electropherograms (i.e., between two peaks and the bridge between them). This method also takes into account the overlap of signals that are responsible for the presence of the peaks and bridge. The developed approach is based on (i) an assumption of the symmetry of peaks if they were not affected by the complex dissociation and (ii) an approximation of the upper boundaries of overlapping zones by quadratic functions. These assumptions allow one to determine all areas in NECEEM electropherograms that are required in a parameter-based approach to calculate the K_d and k_{off} values from the expressions given in relations 4. We tested the accuracy of the method of boundaries positioning in NECEEM by applying it to 33 label-propagation patterns simulated with the exact NECEEM solution. We found that the method's accuracy in the determination of k_{off} and K_d is better than 4% and 15%, respectively, except one simulation that gave a 14% error for k_{off} and four simulations that gave errors in the range of 25%−50% for K_d (from a total of 33 simulations). The developed method for rational boundary determination in NECEEM will facilitate accurate data analysis in this simple and efficient method.

ASSOCIATED CONTENT

Supporting Information. Mathematical derivations, results, and materials and methods. This material is available free of charge via the Internet at http://pubs.acs.org.

AUTHOR INFORMATION

Corresponding Author

*Tel.: 416-736-2100, ext 22345. Fax: 416-736-5936. E-mail: skrylov@yorku.ca.

REFERENCES

(1) (a) Bell, S.; Dutta, A. *Annu. Rev. Biochem.* **2002**, *71*, 333–374. (b) Kohn, K. *Mol. Biol. Cell* **1999**, *10*, 2703–2734. (c) Nooren, I.; Thornton, J. *EMBO J.* **2003**, *22*, 3486–3492. (d) Ullrich, A.; Schlessinger, J. *Cell* **1990**, *61*, 203–212. (e) Vonhippel, P.; Bear, D.; Morgan, W.; McSwiggen *J. Annu. Rev. Biochem.* **1984**, *53*, 389–446.

(2) (a) Hashimoto, M.; Rockenstein, E.; Crews, L.; Masliah, E. *Neuromolecular Med.* **2003**, *4*, 21–36. (b) Prusiner, S. B. *Proc. Natl. Acad. Sci. U.S.A.* **1998**, *95*, 13363–13383.

(3) Wilson, W. D. *Science* **2002**, *295*, 2103–2105.

(4) (a) Hornblower, B.; Coombs, A.; Whitaker, R. D.; Kolomeisky, A.; Picone, S. J.; Meller, A.; Akeson, M. *Nat. Methods* **2007**, *4*, 315–317. (b) Al-Soufi, W.; Reija, B.; Novo, M.; Felekyan, S.; Kuhnemuth, R.;

Seidel, C. A. M. *J. Am. Chem. Soc.* **2005**, *127*, 8775–8784. (c) Li, Y.; Augustine, G. J.; Weninger, K. *Biophys. J.* **2007**, *93*, 2178–2187.

(5) (a) Abdiche, Y. N.; Malashock, D. S.; Pinkerton, A; Pons, J. *Anal. Biochem.* **2008**, *377*, 209–217. (b) Rich, R. L.; Myszka, D. G. *Anal. Biochem.* **2007**, *361*, 1–6.

(6) Berezovski, M.; Krylov, S. N. *J. Am. Chem. Soc.* **2002**, *124*, 13674–13675.

(7) Berezovski, M.; Nutiu, R.; Li, Y.; Krylov, S. N. *Anal. Chem.* **2003**, *75*, 1382–1386.

(8) Okhonin, V.; Krylova, S. M.; Krylov, S. N. *Anal. Chem.* **2004**, *76*, 1507–1512.

(9) (a) Okhonin, V.; Berezovski, M.; Krylov, S. N. *J. Am. Chem. Soc.* **2004**, *126*, 7166–7167. (b) Petrov, A.; Okhonin, V.; Berezovski, M.; Krylov, S. N. *J. Am. Chem. Soc.* **2005**, *127*, 17104–17110. (c) Okhonin, V.; Petrov, A. P.; Berezovski, M.; Krylov, S. N. *Anal. Chem.* **2006**, *78*, 4803–4810.

(10) (a) Okhonin, V.; Berezovski, M. V.; Krylov, S. N. *J. Am. Chem. Soc.* **2010**, *132*, 7062–7068. (b) Cherney, L. T.; Krylov, S. N. *Anal. Chem.* **2011**, *83*, 1381–1387.

(11) (a) Wang, H. L.; Li, T. *Anal. Chem.* **2009**, *81*, 1988–1995. (b) Petrov, A. P.; Cherney, L. T.; Dodgson, B.; Okhonin, V.; Krylov, S. N. *J. Am. Chem. Soc.* **2011**, *133*, 12486−12492.

(12) Yang, P.; Mao, Y.; Lee, A. W.-M.; Kennedy, R. T. *Electrophoresis* **2009**, *30*, 457–464.

(13) (a) Sloat, A. L.; Roper, M. G.; Lin, X; Ferrance, J. P.; Landers, J. P.; Colyer, C. L. *Electrophoresis* **2008**, *29*, 3446–3455. (b) Carrasco-Correa, E. J.; Beneito-Cambra, M.; Herrero-Martinez, J. M.; Ramis-Ramos, G. *J. Chromatogr. A* **2011**, *1218*, 2334–2341. (c) Xu, Y. Z.; Feng, X. J.; Du, W.; Liu, X.; Luo, Q. M.; Liu, B. F. *Anal. Chem.* **2008**, *80*, 6935–6941.

(14) Krylov, S. N. *Electrophoresis* **2007**, *28*, 69–88.

(15) Drabovich, A. P.; Okhonin, V.; Berezovski, M.; Krylov, S. N. *J. Am. Chem. Soc.* **2007**, *129*, 7260–7261.

(16) Krylova, S. M.; Karkhanina, A. A.; Musheev, M. U.; Bagg, E. A. L.; Schofield, C. J.; Krylov, S. N. *Anal. Biochem.* **2011**, *414*, 261–265.

(17) (a) Mendonsa, S. D.; Bowser, M. T. *J. Am. Chem. Soc.* **2004**, *126*, 20–21. (b) Mendonsa, S. D.; Bowser, M. T. *J. Am. Chem. Soc.* **2005**, *127*, 9382–9383. (c) Mosing, R. K.; Mendonsa, S. D.; Bowser, M. T. *Anal. Chem.* **2005**, *77*, 6107–6112. (d) Li, S. F. Y.; Tok, J.; Lai, J.; Leung, T. *Electrophoresis* **2010**, *31*, 2055–2062. (e) Javaherian, S.; Musheev, M. U.; Kanoatov, M.; Berezovski, M. V.; Krylov, S. N. *Nucleic Acids Res.* **2009**, *37*, e62. (f) Kanoatov, M.; Javaherian, S.; Krylov, S. N. *Anal. Chim. Acta* **2010**, *681*, 92–97. (g) Tran, D. T.; Janssen, K. P. F; Pollet, J.; Lammertyn, E.; Anné, J.; Van Schepdael, A.; Lammertyn, J. *Molecules* **2010**, *15*, 1127–1140. (h) Turner, D. J.; Tuytten, R.; Janssen, K. P. F.; Lammertyn, J.; Wuyts, J.; Pollet, J.; Eyckerman, S.; Brown, C.; Kas, K. *Anal. Chem.* **2011**, *83*, 666–670.

(18) (a) Allegri, D.; Mori, G.; Seeber, R. *Analyst* **1996**, *121*, 1359–1365. (b) Shao, X.; Cai, W.; Sun, P.; Zhang, M.; Zhao, G. *Anal. Chem.* **1997**, *69*, 1722–1725. (c) Zhang, Y.; Mo, J.; Xie, T.; Cai, P.; Zou, X. *Anal. Chim. Acta* **2001**, *437*, 151–156.

(19) Goodman, K. J.; Brenna, J. T. *Anal. Chem.* **1994**, *66*, 1294–1301.

(20) Chartier, A.; Georges, J.; Mermet, J. *Chem. Phys. Let.* **1990**, *171*, 347–352.

(21) Parker, C.; Rees, W. *Analyst* **1960**, *85*, 587–600.